Delft University of Technology

Precision in iterative modulation enhanced single-molecule localization microscopy

Kalisvaart, Dylan; Cnossen, Jelmer; Hung, Shih Te; Stallinga, Sjoerd; Verhaegen, Michel; Smith, Carlas S.

Citation (APA)
Kalisvaart, D., Cnossen, J., Hung, S. T., Stallinga, S., Verhaegen, M., & Smith, C. S. (2022). Precision in iterative modulation enhanced single-molecule localization microscopy. *Biophysical Journal*, *121*(12), 2279-2289. https://doi.org/10.1016/j.bpj.2022.05.027

Important note
To cite this publication, please use the final published version (if applicable).
Please check the document version above.

Precision in iterative modulation enhanced single-molecule localization microscopy

Dylan Kalisvaart,[1,*] Jelmer Cnossen,[1] Shih-Te Hung,[1] Sjoerd Stallinga,[2] Michel Verhaegen,[1] and Carlas S. Smith[1,2,*]

[1]Delft Center for Systems and Control, Delft University of Technology, Delft, the Netherlands and [2]Department of Imaging Physics, Delft University of Technology, Delft, the Netherlands

ABSTRACT   Modulation enhanced single-molecule localization microscopy (meSMLM) methods improve the localization precision by using patterned illumination to encode additional position information. Iterative meSMLM (imeSMLM) methods iteratively generate prior information on emitter positions, used to locally improve the localization precision during subsequent iterations. The Cramér-Rao lower bound cannot incorporate prior information to bound the best achievable localization precision because it requires estimators to be unbiased. By treating estimands as random variables with a known prior distribution, the Van Trees inequality (VTI) can be used to bound the best possible localization precision of imeSMLM methods. An imeSMLM method is considered, where the positions of in-plane standing-wave illumination patterns are controlled over the course of multiple iterations. Using the VTI, we analytically approximate a lower bound on the maximum localization precision of imeSMLM methods that make use of standing-wave illumination patterns. In addition, we evaluate the maximally achievable localization precision for different illumination pattern placement strategies using Monte Carlo simulations. We show that in the absence of background and under perfect modulation, the information content of signal photons increases exponentially as a function of the iteration count. However, the information increase is no longer exponential as a function of the iteration count under non-zero background, imperfect modulation, or limited mechanical resolution of the illumination positioning system. As a result, imeSMLM with two iterations reaches at most a fivefold improvement over SMLM at 8 expected background photons per pixel and 95% modulation contrast. Moreover, the information increase from imeSMLM is balanced by a reduced signal photon rate. Therefore, SMLM outperforms imeSMLM when considering an equal measurement time and illumination power per iteration. Finally, the VTI is an excellent tool for the assessment of the performance of illumination control and is therefore the method of choice for optimal design and control of imeSMLM methods.

SIGNIFICANCE   One of the fundamental questions in single-molecule localization microscopy is at what precision the position of a single molecule can be determined. In this work, we show that iterative localization microscopy obtains its precision improvement through incorporation of prior information, thereby reducing the number of photons needed for precise localization. In this situation, the Van Trees inequality quantifies the best possible localization precision that can be achieved. The approach presented here can be generalized to evaluate the best possible localization precision obtainable for different imaging tasks and with different illumination patterns, point spread functions, and/or control strategies.

INTRODUCTION

In single-molecule localization microscopy (SMLM), sparsely activated fluorescent emitters are localized sequentially to obtain a resolution higher than the diffraction limit (1–3). Modulation enhanced SMLM (meSMLM) increases the localization precision using patterned illumination to sparsely activate emitters in a sample, after which emitter

positions are estimated from the sparsity in the emission light (4). Methods such as SIMFLUX (5), SIMPLE (6), and repetitive optical selective exposure (7) use a standing-wave intensity pattern for the illumination, while MINFLUX (8) uses a doughnut-shaped intensity pattern. Axial resolution was also increased through modulated localization (9,10) and axial localization with repetitive optical selective exposure (11), which use patterns with structure in lateral and axial directions.

Localization precision can be increased locally around the emitter by iteratively adapting meSMLM methods through

using prior information on the emitter position that was generated from previous measurements, which we call iterative meSMLM (imeSMLM). In (12), an iterative variant of MINFLUX is discussed, where the position of an emitter is estimated through triangulation with doughnut-shaped illumination patterns. This estimate and its localization uncertainty are used as prior information to reposition and shrink the region of triangulation, after which the emitter position is estimated again. This procedure locally improves precision in the neighborhood of the emitter. Furthermore, it is argued that distributing the limited signal photon budget over many iterations is preferred over increasing the amount of signal photons per iteration, as the information content of signal photons increases over the course of iterations.

To characterize the localization precision of (me)SMLM methods, the Cramér-Rao lower bound (CRLB) is often used (13). Under mild assumptions (see (14)) on the likelihood function of the acquired data, it holds for any unbiased estimator of the parameter vector $\boldsymbol{\theta}$ that $\left(C_{\widehat{\boldsymbol{\theta}}} - I^{-1}(\boldsymbol{\theta}) \right)$ is positive semi-definite. Here, $C_{\widehat{\boldsymbol{\theta}}}$ denotes the estimator covariance, $I(\boldsymbol{\theta})$ is the Fisher information, and $I^{-1}(\boldsymbol{\theta})$ is the CRLB. In particular, the CRLB thus bounds the estimator variance from below. It is shown in (15) that in SMLM, the covariance of the maximum likelihood estimator converges to the CRLB for increasing signal photon counts. As maximum likelihood estimators attain the CRLB asymptotically, the CRLB can be used to quantify the best possible localization precision that can be obtained through (me)SMLM.

imeSMLM methods iteratively update prior information on emitter positions. This prior information locally improves the localization precision during subsequent iterations. Additional prior information can be gained from photoactivation, as is done in iterative MINFLUX (12) or MINSTED (16), as only a pool of molecules is activated. To quantify the best possible improvement of the localization precision in imeSMLM, a suitable error bound should be able to incorporate prior information. The CRLB requires estimators to be unbiased, which means that it is not able to incorporate a prior distribution on the estimands into the localization precision.

In this paper, we use the Van Trees inequality (VTI) as a Bayesian alternative to the CRLB because prior information on the estimands, such as the emitter position, is available. We use the VTI to develop a fundamental limit on the localization precision of imeSMLM methods, for example, where standing-wave illumination patterns are used for the localization. Furthermore, we simulate the effects of illumination pattern positioning on the localization precision. We show that in the absence of background and under perfect modulation, the information content of signal photons increases exponentially as a function of the iteration count. Under non-ideal conditions such as non-zero background or imperfect modulation, this favorable scaling is lost, which shows that optimal design of an imeSMLM method is a complex problem, requiring knowledge of the practical imaging conditions. The VTI is the performance metric of choice to design optimal control strategies in silico.

MATERIALS AND METHODS

In this section, we describe the VTI as a lower bound on the precision of arbitrary estimators in case prior information is available. We describe how to apply the VTI on an imeSMLM method with sinusoidal intensity patterns. Furthermore, we describe the maximum a posteriori (MAP) estimator as a method to iteratively fuse prior information with measurements from the current iteration (see Fig. S1).

VTI

The VTI (17–19) is a Bayesian variant of the CRLB. By treating the estimand vector $\boldsymbol{\theta}$ as a random variable with a known prior distribution, it can incorporate prior information into the localization precision bound. Because of this, the VTI can bound the localization precision of biased and unbiased estimators from below, while the CRLB only bounds the localization precision of unbiased estimators.

The VTI can be used to bound the localization precision of any estimator $\widehat{\boldsymbol{\theta}}$ of the parameter vector $\boldsymbol{\theta}$ from below. For this, the measurements $\boldsymbol{x} \in \mathbb{R}^n$ are modeled as independent realizations from a model distribution, which depends on the parameter vector $\boldsymbol{\theta}$ through the likelihood function $L(\boldsymbol{\theta}|\boldsymbol{x})$. Additionally, a prior distribution $\lambda_{k-1}(\boldsymbol{\theta})$ on the parameter vector is available in each iteration k of the localization procedure (17,18). Under regularity conditions on the likelihood function $L(\boldsymbol{\theta}|\boldsymbol{x})$ and the prior distribution $\lambda_{k-1}(\boldsymbol{\theta})$ (see Note S2), the mean squared error matrix

$$\text{MSE}\left(\widehat{\boldsymbol{\theta}}_k\right) = \mathbb{E}_{\lambda_{k-1}}\left[\int_{\mathbb{R}^n} \left(\widehat{\boldsymbol{\theta}}_k - \boldsymbol{\theta}\right)\left(\widehat{\boldsymbol{\theta}}_k - \boldsymbol{\theta}\right)^T L(\boldsymbol{\theta}|\boldsymbol{x}) \mathrm{d}\boldsymbol{x} \right] \tag{1}$$

of any estimator $\widehat{\boldsymbol{\theta}}_k$ of $\boldsymbol{\theta}$ during iteration k satisfies:

$$\text{MSE}\left(\widehat{\boldsymbol{\theta}}_k\right) - \left(J_{D,k} + J_{P,k}\right)^{-1} \geq 0. \tag{2}$$

Here, $J_k = J_{D,k} + J_{P,k}$ is called the Bayesian information matrix, which is the Bayesian equivalent of the Fisher information matrix. The data information matrix $J_{D,k}$ describes the Fisher information of the data, averaged over the prior. It is given by

$$[J_{D,k}]_{i,j} = \mathbb{E}_{\lambda_{k-1}}\left[[I_k(\boldsymbol{\theta})]_{i,j} \right]. \tag{3}$$

Here, $I_k(\boldsymbol{\theta})$ denotes the Fisher information in iteration k (see Note S1).

The prior information matrix $J_{P,k}$ describes the information contained in the distribution of the prior information. It is given by

$$[J_{P,k}]_{i,j} = \mathbb{E}_{\lambda_{k-1}}\left[\frac{\partial \log(\lambda_{k-1}(\boldsymbol{\theta}))}{\partial \theta_i} \frac{\partial \log(\lambda_{k-1}(\boldsymbol{\theta}))}{\partial \theta_j} \right]. \tag{4}$$

In many practical scenarios, the data information matrix in Eq. 3 is difficult to compute analytically. Aside from certain special cases (see Analytical approximation of Bayesian lower bound on the localization precision), one generally resorts to numerical methods to evaluate the VTI (20,21).

Localization precision for imeSMLM

In imeSMLM, prior information on the emitter position that was generated during previous iterations is used to maximize the information content of signal photons in the next iteration. The CRLB cannot incorporate prior information on estimand vector $\boldsymbol{\theta}$, and therefore the Bayesian VTI is needed.

To be able to formulate the VTI for the described imeSMLM method, a prior distribution on the parameter vector $\boldsymbol{\theta}$ needs to be chosen during each iteration. Here, $\boldsymbol{\theta}$ consists of the emitter position (θ_x, θ_y), the expected signal photon count θ_I, and the expected background photon count per pattern θ_b.

We choose the asymptotic Gaussian distribution of the maximum likelihood estimator as a prior. It is shown in (17,22) that the maximum likelihood estimator asymptotically follows a multivariate normal distribution, with mean $\boldsymbol{\theta}$ and with the covariance given by the CRLB $I^{-1}(\boldsymbol{\theta})$. Alternatively, one can say that for an increasing amount of signal photons, the maximum likelihood estimator becomes unbiased and attains minimum covariance given by the CRLB. As a result of this choice, the VTI for imeSMLM is approximately equal to the CRLB, computed over all iterations (see Fig. S2). This shows that the information increase in imeSMLM is derived from Gaussian prior information.

Using this prior, we iteratively compute the best localization precision as follows (see Fig. S3). In the first iteration, the CRLB $I_1^{-1}(\boldsymbol{\theta})$ is evaluated. The corresponding maximum likelihood estimator $\widehat{\boldsymbol{\theta}}_1$ will approximately be Gaussian distributed, with mean $\boldsymbol{\theta}$ and covariance $I_1^{-1}(\boldsymbol{\theta})$.

We use this distribution as prior information on the next iteration. In iteration 2, we take the prior distribution $\lambda_1(\boldsymbol{\theta})$ to be the probability density function of a multivariate Gaussian distribution. To simulate the best possible localization precision, ignoring the effects of estimation errors made during earlier iterations, the true estimand vector $\boldsymbol{\theta}$ is used as the mean of the Gaussian prior. We then evaluate $J_{D,2}$ and $J_{P,2}$. The new prior $\lambda_2(\boldsymbol{\theta})$ is chosen to be Gaussian, with mean $\boldsymbol{\theta}$ and covariance $(J_{D,2} + J_{P,2})^{-1}$.

In each new iteration k, we take the prior distribution $\lambda_{k-1}(\boldsymbol{\theta})$ to be the probability density function of a multivariate Gaussian distribution, with mean $\boldsymbol{\theta}$ and covariance $(J_{D,k-1} + J_{P,k-1})^{-1}$. We then evaluate $J_{D,k}$ and $J_{P,k}$. The new prior $\lambda_k(\boldsymbol{\theta})$ is chosen to be Gaussian, with mean $\boldsymbol{\theta}$ and covariance $(J_{D,k} + J_{P,k})^{-1}$. This continues until M iterations are completed.

Choice of pattern positions

We consider standing-wave intensity patterns with controllable spatial phase shifts $\phi_{x,k}^{\pm}$ and $\phi_{y,k}^{\pm}$ in two orthogonal orientations. In each iteration of the localization procedure, two x-oriented pattern phases, $\phi_{x,k}^{+}$ and $\phi_{x,k}^{-}$, and two y-oriented pattern phases, $\phi_{y,k}^{+}$ and $\phi_{y,k}^{-}$, are used to illuminate the sample. The superscripts $+$ and $-$ describe the pattern placement with respect to the emitter position. Using prior information on the emitter position, the pattern positions can be selected to maximize the information content of signal photons.

In the initialization step, no prior information is available. Therefore, the pattern positions are chosen to be $\phi_{x,1}^{\pm} = \phi_{y,1}^{\pm} = 0$ by default. A parameter estimate $\widehat{\boldsymbol{\theta}}_1$ is obtained, and the CRLB can now be computed, which results in a $\mathcal{N}(\boldsymbol{\theta}, I_1^{-1}(\boldsymbol{\theta}))$ prior distribution for the next iteration.

If the modulation contrast of the pattern is perfect, the intensity minima of the standing-wave patterns should ideally be placed on the true emitter position (θ_x, θ_y) during subsequent iterations k for the information content of signal photons to be maximal. A similar result was found for iterative MINFLUX, where a doughnut-shaped illumination pattern was used (8,12). This result can be explained intuitively using a thought experiment, as was done in (4). If we assume that the modulation contrast $m = 1$, the intensity minimum has true zero intensity. Suppose that the pattern positions are chosen such that each intensity minimum is placed exactly on the emitter position. As the emitter is illuminated with zero-intensity light, it will not emit any photons. We therefore need to wait infinitely long to receive any non-zero amount of signal photons.

For this to happen, two scenarios are possible. Either the emitter is located perfectly in the intensity minimum or nothing is located in the intensity minimum. The prior information expresses confidence that there is indeed an emitter located in this position, resulting in a decrease of the mean squared error. The prior information thus adds information

to signal photons in case an emitter is illuminated with (near-)zero intensity light.

In practice, the true emitter positions have to be estimated, so this pattern placement cannot be implemented. An implementable pattern placement strategy could replace the true emitter positions with their currently known estimates $\widehat{\theta}_{x,k-1}$ and $\widehat{\theta}_{y,k-1}$. However, this can cause the localization precision to become sensitive to estimation errors. If the current position estimate is imprecise, intensity minima will be placed away from the true emitter position, and the newly obtained prior distribution will add little information.

To decrease the sensitivity to estimation errors of the iterative localization method, the intensity minima of two patterns, ϕ_k^{+} and ϕ_k^{-}, can be placed symmetrically around the current estimate of the emitter position, as shown in Fig. 1 (also see Fig. S4). In each iteration, the distance between the intensity minima is decreased, thereby locally improving the localization precision around the current estimate of the emitter position.

In this article, we consider a pattern position control strategy where illumination minima are placed symmetrically around the current estimate of the emitter position, in which the distance between the emitter position and an intensity minimum scales with the localization precision of the previous iteration. This control strategy is given by

$$
\begin{cases}
\phi_{x,k}^{\pm} = \omega\left(\widehat{\theta}_{x,k-1} \pm \alpha\sigma_{x,k-1}\right) - \pi, \\
\phi_{y,k}^{\pm} = \omega\left(\widehat{\theta}_{y,k-1} \pm \alpha\sigma_{y,k-1}\right) - \pi.
\end{cases}
\tag{5}
$$

Here, ω denotes the spatial pattern frequency. As the illumination pattern is at best diffraction limited, it must hold that $\omega \leq 2\pi \cdot \frac{2\mathrm{NA}}{\lambda_{\mathrm{ex}}}$, where λ_{ex} is the excitation wavelength and NA is the numerical aperture. The localization precisions $\sigma_{x,k-1}$ and $\sigma_{y,k-1}$ are the square roots of the first and second diagonal elements of J_{k-1}^{-1}, respectively. The aggressiveness parameter α determines how close the pattern minima are placed to the estimated emitter position.

MAP estimation

Estimators used for iterative localization microscopy should be able to recursively fuse measurements with prior knowledge on estimands that was obtained during earlier iterations. In each iteration k, we compute the MAP estimator $\widehat{\boldsymbol{\theta}}_k$, which is given by the maximizing argument of the posterior distribution $p(\boldsymbol{\theta}|\boldsymbol{x}_1, \ldots, \boldsymbol{x}_k)$. As the measurements $\boldsymbol{x}_1, \ldots, \boldsymbol{x}_k$ are independent, the posterior satisfies the following recursion:

$$
\begin{aligned}
p(\boldsymbol{\theta}|\boldsymbol{x}_1, \ldots, \boldsymbol{x}_k) &\overset{\boldsymbol{\theta}}{\propto} p(\boldsymbol{x}_k|\boldsymbol{\theta})p(\boldsymbol{\theta}|\boldsymbol{x}_1, \ldots, \boldsymbol{x}_{k-1}) \\
&\overset{\boldsymbol{\theta}}{\propto} p(\boldsymbol{x}_k|\boldsymbol{\theta})p(\boldsymbol{x}_1, \ldots, \boldsymbol{x}_{k-1}|\boldsymbol{\theta})p(\boldsymbol{\theta}).
\end{aligned}
\tag{6}
$$

Here, $p(\boldsymbol{\theta}|\boldsymbol{x}_1, \ldots, \boldsymbol{x}_{k-1})$ denotes the posterior from the previous iteration, $p(\boldsymbol{x}_k|\boldsymbol{\theta})$ represents the likelihood of the measurements from the current iteration, and $p(\boldsymbol{x}_1, \ldots, \boldsymbol{x}_{k-1}|\boldsymbol{\theta})$ represents the likelihood of the accumulated measurements from previous iterations. If prior information is available, such as in photoactivation (12,16), it can be included in $p(\boldsymbol{\theta})$. To keep the analysis as general as possible, we choose $p(\boldsymbol{\theta})$ to be a uniform (improper) prior over $\mathbb{R}^4$ to represent the lack of prior information on $\boldsymbol{\theta}$ before measurements are done. For this choice, the estimation error of the MAP estimator is guaranteed to converge to the VTI if the likelihood reflects the underlying distribution of the data. The MAP estimate can then be computed as follows:

$$
\widehat{\boldsymbol{\theta}}_k = \arg\max_{\boldsymbol{\theta}} \left[\log(p(\boldsymbol{x}_1, \ldots, \boldsymbol{x}_{k-1}|\boldsymbol{\theta})) + \log(p(\boldsymbol{x}_k|\boldsymbol{\theta}))\right].
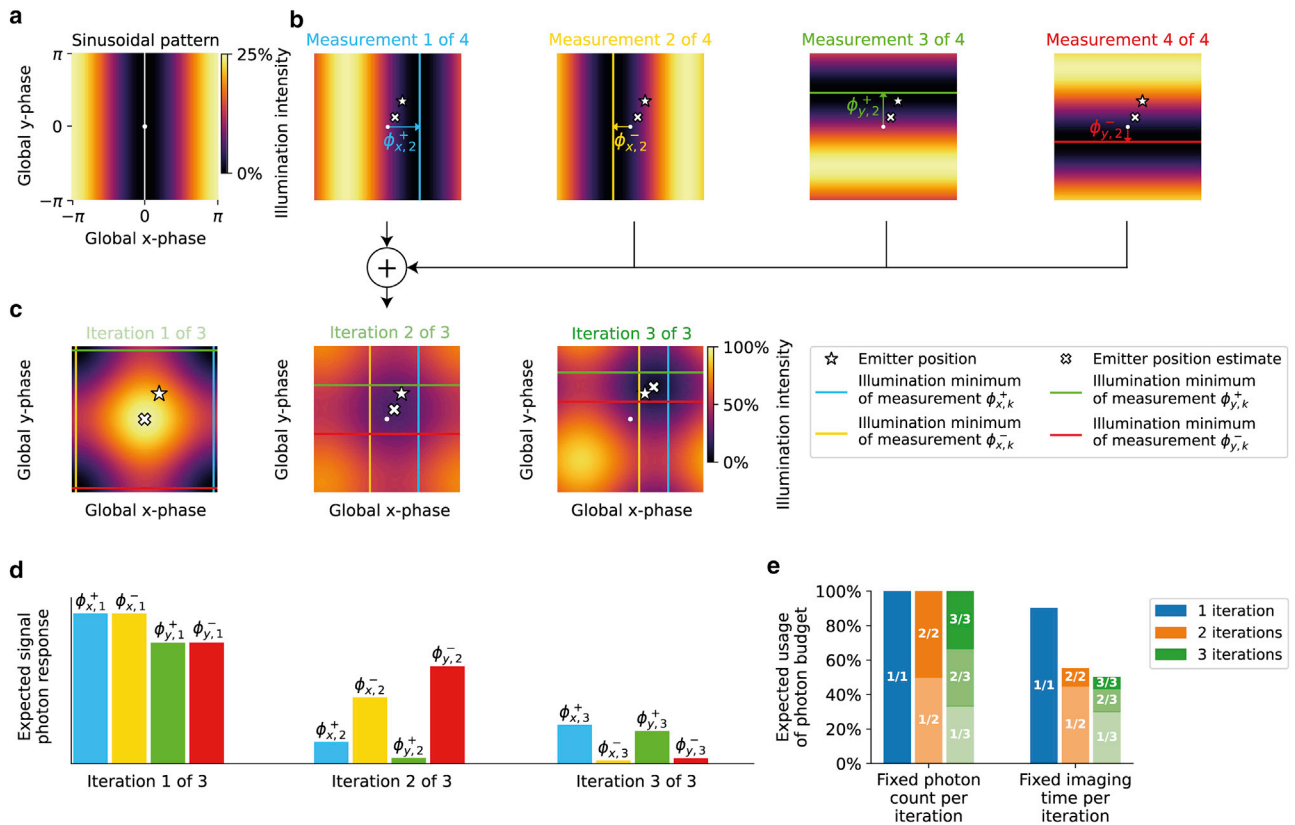\tag{7}
$$

FIGURE 1 Pattern position control strategy (see Eq. 5) to iteratively increase information content of signal photons. (*a*) Example of one period of a sinusoidal intensity pattern in the *x*-direction, with the intensity minimum centered at a global phase zero. (*b*) Individual illumination patterns placed during iteration 2. In each iteration, four sinusoidal illumination patterns are placed, such that current estimate of the emitter position is enclosed between the illumination minima of the patterns. (*c*) Summed illumination patterns over the course of three iterations. The distance between the intensity minimum of the summed patterns and the emitter position reduces iteratively as a result of adjusting the search region based on prior information about the achieved precision in the previous iteration. (*d*) Expected signal photon response from the emitter in (*b*) and (*c*) over the course of three iterations, using the illumination placement from (*c*). (*e*) Illustration of the expected signal photon budget for one, two, and three iterations. Two scenarios are considered in this article, namely the case where the signal photon count is kept constant over the course of all iterations and the case where the imaging time and illumination intensity are kept constant over the course of all iterations. In the latter case, the signal photon budget is only exhausted by imeSMLM in case the single emitter is illuminated with maximum intensity during all iterations. If the intensity pattern minima are placed close to the emitter, a reduced number of photons is recorded within the same time window.

Simulations and parameter values

The VTI and MAP estimates for the described imeSMLM method were obtained using representative in silico experiments. The VTI was evaluated using simple Monte Carlo integration (see Note S3), where 50,000 Monte Carlo samples were used for convergence. 50,000 realizations of regions of interest were simulated by realizing the image formation model (see Note S1), where the emitter was located in the center of the camera pixel array and where its subpixel position was uniformly randomized. MAP estimates were obtained from Eq. 7 using Levenberg-Marquardt optimization (23,24). The model parameters (see Table S1) are considered to be representative of an imeSMLM experiment where standing-wave intensity patterns are used to illuminate the sample. We choose the pattern frequency ω and the standard deviation of the Gaussian point spread function (PSF) to be diffraction limited. This maximizes the information contained in the illumination pattern. For the chosen parameters, the pattern pitch is approximately equal to twice the standard deviation of the Gaussian PSF. This is consistent with earlier work on modulation enhanced localization microscopy with sinusoidal illumination (5).

Software and data availability

The software for computing the VTI, simulating regions of interest, and estimating emitter positions is available at (25). The unprocessed simulated data underlying the results are available at (26).

RESULTS AND DISCUSSION

In this section, we present the theoretical and numerical results of this study. We describe a closed-form expression of the VTI, assuming one-dimensional localization, no image discretization by the camera, and zero background. Simulations explore the effects of the number of iterations and the choice of pattern positioning on the localization precision. In Figs 2 and 3, the effects of the iteration count and pattern positioning on the localization precision are simulated, respectively assuming a fixed photon count per iteration
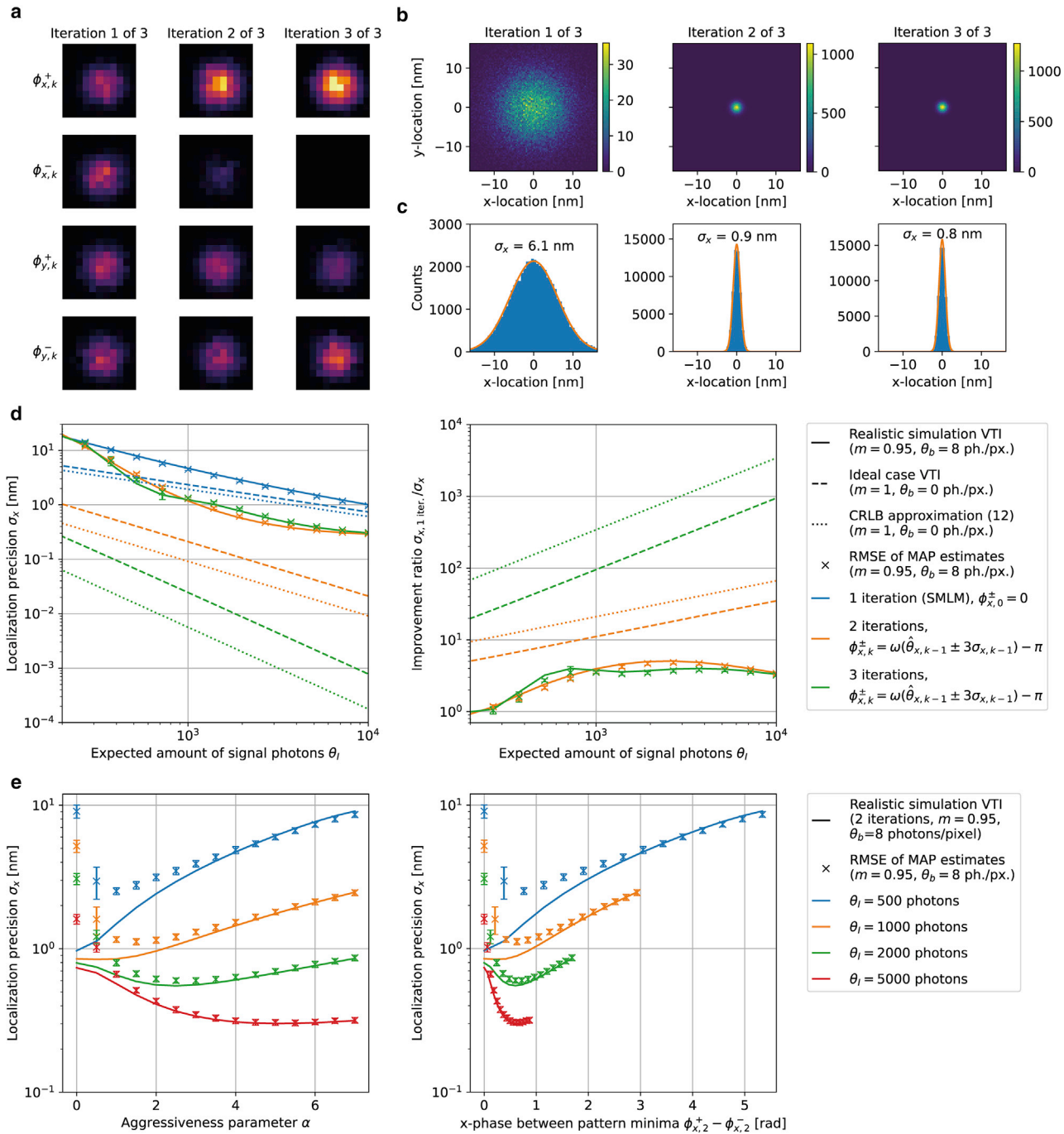
FIGURE 2 Simulated iterative localization and precision bound using a fixed expected signal photon budget per iteration. In (a)–(d), the pattern positioning of Eq. 5 was used with aggressiveness parameter $\alpha = 3$. In (d) and (e), the results are compared with the theoretical limit of Eq. 9 and the precision approximation of Eq. 10, which assume perfect modulation and zero background. Error bars denote the standard deviation of the root-mean-square error, obtained by comparing 200 batches of 250 MAP estimates. (a) Example of simulated regions of interest during three iterations of an iterative localization experiment. Contrast was enhanced for visualization purposes. The divergence in emitter intensity from iteration 1 to iteration 3 is the result of shrinking the distance between pattern minima while enforcing a fixed expected signal photon budget per iteration in simulation. As a result, the pattern minima that are placed furthest from the emitter position (due to position estimation errors in the previous iteration) will use a larger share of the signal photon budget. (b) Two-dimensional histogram of MAP localizations on 50,000 simulated regions of interest during three iterations of an iterative localization experiment at an expected signal photon count of $\theta_I = 2000$ photons. (c) Histogram of MAP localizations projected on the x-direction. A Gaussian with standard deviation σ_x is fitted on the histogram. (d) Simulated localization precision in x-direction as a function of the expected signal photon count when one, two, or three iterations are used. (e) Simulated localization precision in x-direction as a function of the aggressiveness parameter α, and the distance between the pattern minima using the same values of the aggressiveness parameter α, for different expected signal photon counts and assuming a constant signal photon count per iteration.
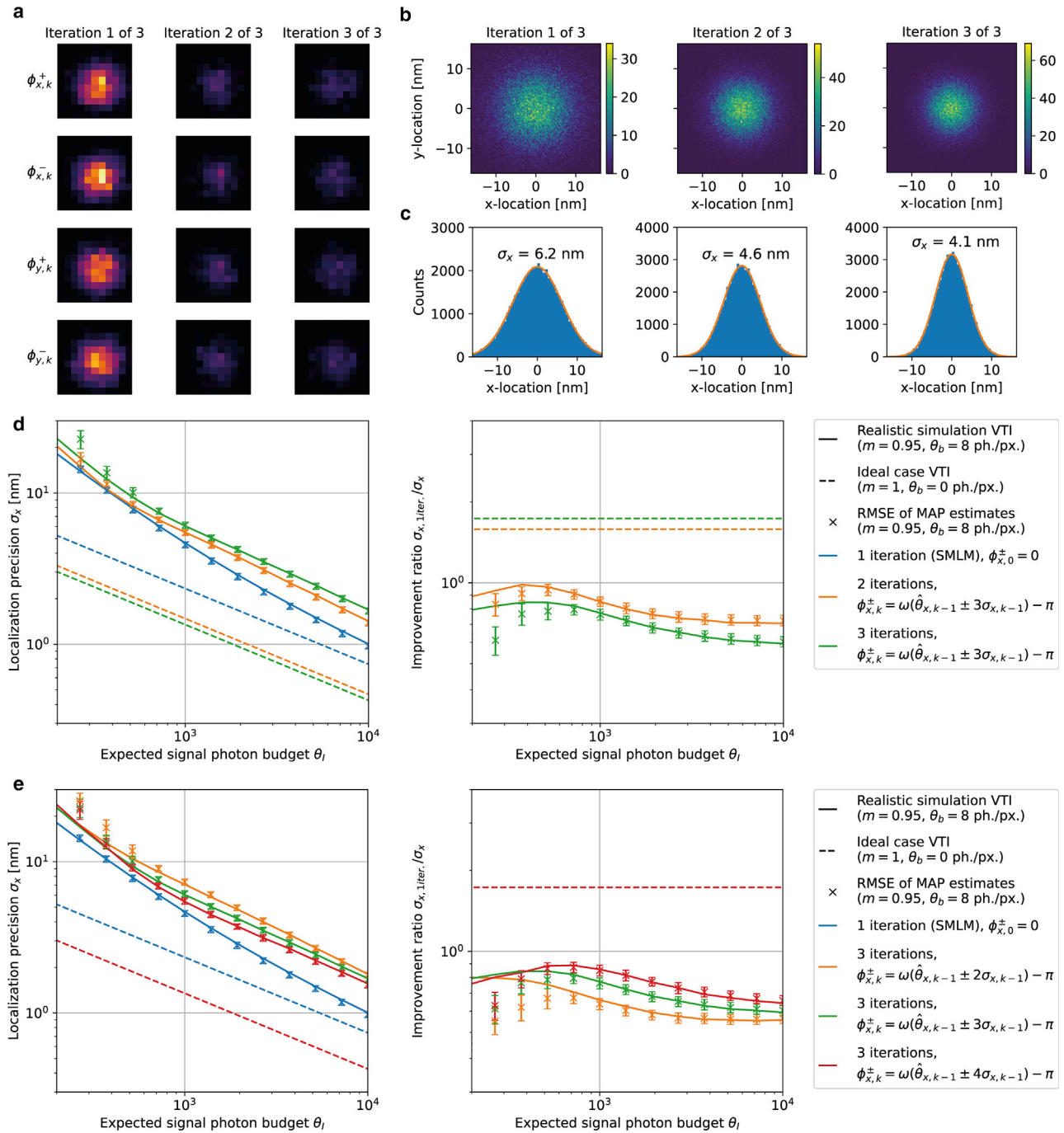
FIGURE 3 Simulated iterative localization and precision bound using a fixed imaging time and illumination power per iteration. In (*a*)–(*d*), the pattern positioning of Eq. 5 was used with aggressiveness parameter $\alpha = 3$. In (*d*) and (*e*), results are compared with the theoretical limit of Eq. 9, which assumes perfect modulation and zero background. Error bars denote the standard deviation of the root-mean-square error, obtained by comparing 200 batches of 250 MAP estimates. (*a*) Example of simulated regions of interest during three iterations of an iterative localization experiment. Contrast was enhanced for visualization purposes. (*b*) Two-dimensional histogram of MAP localizations on 50,000 simulated regions of interest during three iterations of an iterative localization experiment at an expected signal photon budget of $\theta_I = 2000$ photons. (*c*) Histogram of MAP localizations projected on the *x*-direction. A Gaussian with standard deviation σ_x is fitted on the histogram. (*d*) Simulated localization precision in *x*-direction as a function of the expected signal photon budget θ_I, when one, two, or three iterations are used. (*e*) Simulated localization precision in *x*-direction as a function of the expected signal photon budget for different pattern positioning strategies.

and a fixed imaging time and illumination power per iteration.

Analytical approximation of Bayesian lower bound on the localization precision

Under some assumptions on the image formation model, analytical expressions for the localization precision can be derived using the VTI. We derive an analytical approximation of the Bayesian VTI on the localization precision of an imeSMLM method where sinusoidal intensity patterns are used, given a Gaussian PSF and a sequence of pattern positions.

We limit ourselves to one-dimensional localization where we disregard the effect of discretization of the image due to the finite size of camera pixels. In addition, we do not estimate the expected signal photon count θ_I, and we ignore background such that $\theta_b = 0$. Under these assumptions, the derived analytical approximation serves as a fundamental limit on the localization precision. That is, the localization precision of the described imeSMLM method for two-dimensional localization, under the effects of image discretization, estimation uncertainty on θ_I and θ_b, and non-zero background, can only be worse than the analytical approximation.

The approximation of the best possible localization precision is given by (see Note S4):

$$\sigma_{x,k} \geq (J_k)^{-\frac{1}{2}} \geq \frac{\sigma_{x,k-1}}{\sqrt{1 + \sigma_{x,k-1}^2 (F_{\text{PSF}} + F_{\text{illum}})}}, \tag{8a}$$

$$F_{\text{PSF}} = \frac{\theta_I c_k}{\sigma_{\text{PSF}}^2} \left(2 + \left(m \cos\left(\omega \widehat{\theta}_{x,k-1} - \phi_{x,k}^+\right) \right. \right.$$
$$\left. \left. + m \cos\left(\omega \widehat{\theta}_{x,k-1} - \phi_{x,k}^-\right) \right) \exp\left(-\frac{\omega^2 \sigma_{x,k-1}^2}{2} \right) \right), \tag{8b}$$

$$F_{\text{illum}} = \theta_I c_k \omega^2 \left(2 - \left(m \cos\left(\omega \widehat{\theta}_{x,k-1} - \phi_{x,k}^+\right) \right. \right.$$
$$\left. \left. + m \cos\left(\omega \widehat{\theta}_{x,k-1} - \phi_{x,k}^-\right) \right) \exp\left(-\frac{\omega^2 \sigma_{x,k-1}^2}{2} \right) \right). \tag{8c}$$

Here, c_k models the expected photon count per iteration under imperfect illumination (see Note S1). Furthermore, σ_{PSF} denotes the standard deviation of a Gaussian PSF, and m denotes the modulation contrast of the illumination pattern. In the denominator, the term "1" accounts for the prior information. The terms F_{PSF} and F_{illum} describe the information derived from the spot center estimation and the information derived from the illumination pattern modulation, respectively. Note that Eq. 8 is an exact representation

of the VTI for $m = 1$ and $\phi_{x,k}^+ = \phi_{x,k}^-$ and a lower bound on the VTI for $m < 1$ or $\phi_{x,k}^+ \neq \phi_{x,k}^-$.

If the pattern positions of Eq. 5 are substituted into Eq. 8, we obtain:

$$\sigma_{x,k} \geq (J_k)^{-\frac{1}{2}} \geq \frac{\sigma_{x,k-1}}{\sqrt{1 + \sigma_{x,k-1}^2 (F_{\text{PSF}} + F_{\text{illum}})}}, \tag{9a}$$

$$F_{\text{PSF}} = \frac{\theta_I c_k}{\sigma_{\text{PSF}}^2} \left(2 - 2m \cos(\omega \alpha \sigma_{x,k-1}) \exp\left(-\frac{\omega^2 \sigma_{x,k-1}^2}{2} \right) \right), \tag{9b}$$

$$F_{\text{illum}} = \theta_I c_k \omega^2 \left(2 + 2m \cos(\omega \alpha \sigma_{x,k-1}) \exp\left(-\frac{\omega^2 \sigma_{x,k-1}^2}{2} \right) \right). \tag{9c}$$

Assuming that the modulation contrast is perfect and that zero background photons are recorded, Eq. 9 can be used to derive the optimal distribution of the signal photon budget (see Note S5). This proves that it is optimal to isotropically distribute the signal photon budget over the number of iterations from iteration 2 onwards.

From Eq. 9 with $m = 1$, it can be seen that the contribution of the expected signal photon count θ_I to the localization precision grows exponentially as $\sigma_{x,k-1}$ decreases. This implies that the information content per signal photon grows as the number of iterations increases. Assuming that the modulation contrast is perfect and that zero background photons are recorded, it is thus favorable to increase the number of iterations as much as possible within the limited photon budget.

However, increasing the number of iterations results in a lower amount of signal photons per iteration, lowering the signal-to-background ratio in each iteration. The exponential scaling is therefore destroyed by background. Furthermore, we assume here that the mechanical resolution of the illumination positioning system is not limiting, such that every illumination-pattern position between $-\pi$ and π can be reached. In practice, this becomes increasingly difficult for small $\sigma_{x,k-1}$, preventing the exponential limit to be reached for high amounts of iterations. Because of these factors, it makes sense to limit the number of iterations in practical applications.

Effect of iterations on localization precision

From the theoretical limit of Eq. 8, it was found that illumination pattern control can exponentially increase the information content of signal photons under perfect modulation and zero background, making an increase of the iteration count preferable over an increase of the number of photons per iteration. The effect of the iteration count and pattern

positioning on the localization precision for imperfect modulation and zero background will be simulated in this subsection.

In Fig. 2, the effect of the iteration count on the localization precision is simulated assuming a fixed expected signal photon count per iteration. The aggressiveness parameter α was set to 3 for these simulations. For each simulation, the VTI was evaluated, and MAP estimates were computed for 50,000 randomly generated regions of interest (see Note S1). These results are compared with the theoretical limit of Eq. 8, where we assume perfect modulation to reflect the best achievable localization precision. We also compute the CRLB reported in (12), where the illumination minimum is approximated by a quadratic profile. Assuming that N signal photons are collected during each iteration, this approximation of the CRLB is given by

$$\sigma_{x,k} \gtrsim \frac{\left| \phi_{x,k}^{+} - \phi_{x,k}^{-} \right|}{4\omega N^{1/2}} = \frac{2\alpha\sigma_{x,k-1}}{4N^{1/2}}. \qquad (10)$$

In Fig. 2 a, examples of simulated regions of interest are shown assuming a fixed expected signal photon count per iteration. From iterations 1 to 3, the emitter intensity appears to diverge. This effect is caused by enforcing a fixed expected signal photon budget per iteration in simulation. Due to this assumption, the emitter intensities represent the share of the expected signal photon budget used during each measurement. As the distance between pattern minima shrinks over the course of iterations, the signal photon budget is distributed increasingly unevenly over the measurements.

In iteration 1, pattern minima are placed far from the true emitter position, so the emitter is illuminated with high intensity from all patterns. As such, the illumination patterns will use an approximately equal share of the signal photon budget.

In subsequent iterations, pattern minima are placed increasingly close to the estimated emitter position. Because we make an estimation error, pattern minima are placed asymmetrically around the true emitter position. As a result, the pattern minima that are placed furthest from the emitter position will use a larger share of the signal photon budget. As the expected signal photon budget is constant over the iterations, the emitter intensities appear to diverge.

From Fig. 2 d, it can be seen that iterative localization using the pattern placement of Eq. 5 results in improved localization precision over SMLM. For eight background photons per pixel and 95% modulation, we found that around a fivefold improvement over SMLM can be reached by doing two iterations at a signal photon count of 644 signal photons per iteration. When doing three iterations, the maximum improvement over SMLM is around four, reached at 240 signal photons per iteration.

These findings are in contrast with the results under perfect modulation and zero background, as described by the analytical approximation. As expected from the earlier analysis, we find that the localization precision is proportional to θ_I^{-1} when doing two iterations and $\theta_I^{-3/2}$ when doing three iterations. This difference is explained by the fact that the precision loss due to background, imperfect modulation, and discretization accumulates as the number of iterations increases, as the lowered precision $\sigma_{x,k-1}$ in a previous iteration is carried over to the next iteration. In practice, the favorable exponential increase of information over the course of the iterative procedure is thus lost.

When recording 315 or more photons per iteration, using two iterations rather than three results in a better localization precision. To investigate the cause, Fig. S5 shows the localization precision as a function of the cumulative signal photon count at a total signal photon count of 2000 photons. For eight background photons per pixel and 95% modulation, we see that using three iterations is still preferred when the second out of three iterations ends at 1333 signal photons. At this moment, using three iterations results in a 4.5-fold precision increase over using SMLM. During the third out of three iterations, the localization precision improves only marginally, resulting in a decrease of the precision improvement to 3.7 with respect to SMLM. This is not expected from the analytical approximation under perfect modulation and zero background, where the localization precision improvement over SMLM increases from 13 to 190 during the third iteration.

Simulations show similar results for different settings of the modulation contrast and the background count. Specifically, we find a stagnation of the localization precision during the third iteration for 80% and 90% modulation contrast (see Fig. S6) and background counts of 1, 4, and 12 photons per pixel (see Fig. S7), in contrast to the results for perfect modulation and zero background.

We can conclude that imperfect modulation and non-zero background limit the best possible localization precision when the illumination pattern minima are placed closer to the emitter position. When distributing photons equally over the iterations, increasing the number of iterations indefinitely does not necessarily lead to increasingly informative signal photons.

Additionally, we see ill-convergence of the MAP estimator at perfect modulation when patterns are placed close to the true emitter position (see Figs. S6 and S10). This is caused by a (near-)zero signal photon response under perfect modulation. For pattern minima that are close to the true emitter position, the signal photon response is low or zero for perfect modulation. This causes low signal-to-background ratios, which means that the shape of the PSF is poorly represented in the data. Analogous to existing results on the maximum likelihood estimator (15), the MAP estimator fails to consistently estimate the emitter position with minimum uncertainty. For 95% modulation, we do not see ill-convergence for expected background counts of one or more photons per pixel, although the maximum

localization precision is not reached for $\alpha < 2$ due to the low signal-to-background ratio (see Fig. S11).

In the simulations of Fig. 2 *d*, the aggressiveness parameter α was kept constant at three. For zero background and perfect modulation, it is expected that reducing the aggressiveness improves the localization precision independently from the expected signal photon budget (see Fig. S8). For eight background photons per pixel and 95% modulation, we see that $\alpha = 2$ improves the localization precision fourfold over SMLM when recording 518 signal photons.

The optimal choice of the aggressiveness parameter depends on the expected background photon count, the modulation contrast, and the expected signal photon count. Fig. 2 *e* shows that the optimal α decreases for a decreasing signal photon count (see Fig. 2 *e*). For 95% modulation and eight background photons per pixel, $\alpha = 2.5$ is optimal at a signal photon budget of 2000 photons, while $\alpha = 5.5$ is optimal at a signal photon budget of 5000 photons. We also see that the optimal α decreases for increasing background (see Fig. S11). That is, as the signal-to-background ratio increases, the optimal α increases as well.

For perfect modulation, we have already argued that the localization precision can be optimized by placing pattern minima directly on the emitter. However, this optimum shifts when the modulation contrast is imperfect (see Fig. S10). Specifically, this shows that the localization precision does not improve from infinitely reducing the distance between pattern minima in case the pattern modulation is imperfect. This indicates that the prediction from (8) does not hold for imperfect modulation.

Therefore, a practical way of choosing α is needed to optimize imeSMLM. If prior knowledge about the signal photon count, the background, and the modulation contrast is available, the theoretically optimal α should be found by optimizing the VTI. It remains an open question how to do this systematically. A practical solution could be to choose α from a lookup table, constructed in silico from optimizing the VTI under a range of practical experimental conditions.

In Fig. 3, the effect of the iteration count and pattern positioning on the localization precision is simulated, assuming a fixed imaging time and illumination power per iteration. As a consequence of using patterned illumination, the use of the available signal photon budget varies between iterations (see Fig. 1 *e*). Identically to the previous simulations, the aggressiveness parameter α was set to three, and the MAP estimates were computed for 50,000 regions of interest.

From Fig. 3 *d* and *e*, we see that SMLM outperforms imeSMLM over a range of signal photon budgets and for different pattern positioning strategies. For eight background photons per pixel and 95% modulation, SMLM outperforms imeSMLM with three iterations by a factor 1.2 at a signal photon budget of 518 signal photons.

To investigate the cause of this performance loss, we simulate the localization precision per recorded photon under the illumination strategy of Eq. 5 (see Fig. S9 *a*

and *c*). It can be seen that imeSMLM still enables an increase of the information content per recorded signal photon. For eight background photons per pixel and 95% modulation, the localization precision is improved 1.4-fold over SMLM when the first 411 signal photons are recorded using two iterations. When doing three iterations, the maximum improvement over SMLM is 1.5, reached after 422 signal photons.

However, SMLM uses more of the available signal photon budget within the same time span, ultimately resulting in a better localization precision over imeSMLM (see Fig. S9 *b* and *d* in the Supporting Material). For SMLM, all 2000 signal photons within the budget are collected. For imeSMLM, all signal photons available in first iteration are collected, as the illumination intensity equals that of SMLM. In subsequent iterations, pattern minima are placed closer to the emitter position, resulting in a reduced signal photon response. When doing three iterations in total, 60 signal photons are collected on average during the second iteration, and 40 signal photons are collected on average during the third iteration. While these photons are more informative than those obtained with SMLM, the total amount of information is not enough to outperform SMLM.

These effects are further exemplified by the analytical approximation, as pattern minima are placed even closer to the emitter position when the effects of background and imperfect modulation are removed. For three iterations with a photon budget of 2000 photons, eight signal photons are collected on average during the second iteration, and one signal photon is collected on average during the third iteration. As the amount of signal photons with increased information is so limited, the localization precision approximately scales with $\theta_I^{-1/2}$ for imeSMLM, with a constant improvement factor of 1.6 over SMLM when doing two iterations and 1.7 when doing three iterations.

In the simulations of Fig. 3 *d*, the aggressiveness parameter α was kept constant at three. Fig. 3 *e* shows that for zero background and perfect modulation, it is expected that the aggressiveness does not significantly influence the maximum localization precision, as on average less than 15 signal photons are collected during the second and third iterations for $\alpha = 2$, 3, or 4. As such, the precision improvement from aggressive localization is balanced by a reduction of the signal photon count. For eight background photons per pixel and 95% modulation, we see that aggressive localization with $\alpha = 2$ results in a 1.3- to 1.8-fold reduction in localization precision for signal photon budgets θ_I between 200 and 10,000 photons.

CONCLUSIONS

In imeSMLM, resolution is improved locally around an emitter position by using prior information that was derived from measurements in earlier iterations. The CRLB cannot incorporate prior information, as it requires estimators to be

unbiased. By treating estimands as random variables with a known prior distribution, the Bayesian VTI can be used to bound the maximally achievable localization precision from below. The VTI is useful for bounding the localization precision in imeSMLM as it is able to account for the effect of prior information that is generated over the course of iterations.

We derived an analytical approximation of the Bayesian lower bound on the localization precision of imeSMLM methods that make use of standing-wave illumination patterns in the absence of image discretization by the camera, estimation uncertainty on the signal photon count, and background fluorescence. This fundamental limit cannot be surpassed, as relaxing the aforementioned assumptions can only worsen the localization precision of imeSMLM methods. Using this limit, we have shown that the information content of signal photons increases exponentially as a function of the iteration count when the modulation contrast is 100%. Additionally, we prove that for perfect modulation, it is optimal to isotopically distribute the single-molecule's photon budget over the number of iterations from iteration 2 onwards.

We demonstrate a practical imeSMLM pattern control strategy using the VTI. The VTI was simulated to assess the performance of imeSMLM under eight photons per pixel background and 95% modulation contrast. By using two iterations in total, imeSMLM reaches at most a five-fold improvement over SMLM. This indicates that the exponential localization improvement as a function of the iteration count cannot be achieved in most experiments, as it breaks down for slight imperfections in the modulation contrast.

Moreover, SMLM is able to outperform imeSMLM in case the imaging time and illumination laser power are kept constant between iterations. imeSMLM results in signal photons with increased information content. However, placing pattern minima close to the emitter position reduces the signal photon response, while SMLM is able to collect more signal photons within the same time frame. At a signal photon budget of 2000 photons, we find that SMLM is around 1.2 times better than three iterations of imeSMLM at eight expected background photons per pixel and 95% modulation contrast. We conclude that imeSMLM is able to increase the information content per signal photon but that this information increase does not necessarily outweigh the reduced signal photon response.

From this, we find that the optimal selection of pattern placement, the number of iterations, and the time spent per iteration in imeSMLM depends on many factors, such as the photon budget, imperfections in the illumination system, and the expected background count. Specifically, we show that the smallest step size is most likely not the best one and that the optimal step size depends on the molecule intensity, modulation contrast, and background fluorescence. Furthermore, we demonstrate that the localization precision only scales with the step size over a small set of experimental conditions.

The VTI can be used to quantify the best possible performance of illumination pattern control strategies and is therefore a promising performance metric in optimal control of imeSMLM methods. In this article, we chose to analyze imeSMLM with four sinusoidal illumination patterns. This is the most straightforward approach using sinusoidal illumination. It remains an open question if other arrangements of sinusoidal illumination patterns could lead to further imeSMLM improvements. Other illumination pattern shapes, such as the doughnut-shaped pattern from MINFLUX ([8],[12]), could also lead to improvements in imeSMLM. When designing imeSMLM experiments, the VTI is the preferred tool to tailor the pattern placement strategy to different imaging conditions.

SUPPORTING MATERIAL

Supporting material can be found online at https://doi.org/10.1016/j.bpj.2022.05.027.

AUTHOR CONTRIBUTIONS

D.K., S.H., and C.S.S. designed the research. D.K. and J.C. wrote the simulation code. D.K. carried out the simulations, analyzed the data, and wrote the manuscript, which was edited by C.S.S., S.S., and M.V. The study was supervised by C.S.S.

ACKNOWLEDGMENTS

DECLARATION OF INTERESTS

The authors declare no competing interests.

SUPPORTING CITATIONS

References ([27],[28]) appear in the supporting material.

REFERENCES

1. Betzig, E., G. H. Patterson, R. Sougrat, O. W. Lindwasser, S. Olenych, J. S. Bonifacino, M. W. Davidson, J. Lippincott-Schwartz, and H. F. Hess. 2006. Imaging Intracellular fluorescent proteins at nanometer resolution. *Science.* 313:1642–1645. https://doi.org/10.1126/science.1127344.

2. Rust, M. J., M. Bates, and X. Zhuang. 2006. Sub-diffraction-limit imaging by stochastic optical reconstruction microscopy (STORM). *Nat. Methods.* 3:793–796. https://doi.org/10.1038/nmeth929.

3. Huang, B., M. Bates, and X. Zhuang. 2009. Super-resolution fluorescence microscopy. *Annu. Rev. Biochem.* 78:993–1016. https://doi.org/10.1146/annurev.biochem.77.061906.092014.

4. Reymond, L., T. Huser, V. Ruprecht, and S. Wieser. 2020. Modulation-enhanced localization microscopy. *J. Phys. Photonics.* 2:041001. https://doi.org/10.1088/2515-7647/ab9eac.

5. Cnossen, J., T. Hinsdale, R. Ø. Thorsen, M. Siemons, F. Schueder, R. Jungmann, C. S. Smith, B. Rieger, and S. Stallinga. 2019. Localization microscopy at doubled precision with patterned illumination. *Nat. Methods.* 17:59–63. https://doi.org/10.1038/s41592-019-0657-7.

6. Reymond, L., J. Ziegler, C. Knapp, F.-C. Wang, T. Huser, V. Ruprecht, and S. Wieser. 2019. SIMPLE: structured illumination based point localization estimator with enhanced precision. *Opt Express.* 27:24578–24590. https://doi.org/10.1364/oe.27.024578.

7. Gu, L., Y. Li, S. Zhang, Y. Xue, W. Li, D. Li, T. Xu, and W. Ji. 2019. Molecular resolution imaging by repetitive optical selective exposure. *Nat. Methods.* 16:1114–1118. https://doi.org/10.1038/s41592-019-0544-2.

8. Balzarotti, F., Y. Eilers, K. C. Gwosch, A. H. Gynnå, V. Westphal, F. D. Stefani, J. Elf, and S. W. Hell. 2017. Nanometer resolution imaging and tracking of fluorescent molecules with minimal photon fluxes. *Science.* 355:606–612. https://doi.org/10.1126/science.aak9913.

9. Jouchet, P., C. Cabriel, N. Bourg, M. Bardou, C. Poüs, E. Fort, and S. Lévêque-Fort. 2021. Nanometric axial localization of single fluorescent molecules with modulated excitation. *Nat. Photonics.* 15:297–304. https://doi.org/10.1038/s41566-020-00749-9.

10. Jouchet, P., C. Cabriel, N. Bourg, M. Bardou, C. Poüs, E. Fort, and S. Lévêque-Fort. 2020. In depth 3D single molecule localization microscopy with time modulated excitation. *Biophys. J.* 118:149a. https://doi.org/10.1016/j.bpj.2019.11.933.

11. Gu, L., Y. Li, S. Zhang, M. Zhou, Y. Xue, W. Li, T. Xu, and W. Ji. 2021. Molecular-scale axial localization by repetitive optical selective exposure. *Nat. Methods.* 18:369–373. https://doi.org/10.1038/s41592-021-01099-2.

12. Gwosch, K. C., J. K. Pape, F. Balzarotti, P. Hoess, J. Ellenberg, J. Ries, and S. W. Hell. 2020. MINFLUX nanoscopy delivers 3D multicolor nanometer resolution in cells. *Nat. Methods.* 17:217–224. https://doi.org/10.1038/s41592-019-0688-0.

13. Ober, R. J., S. Ram, and E. S. Ward. 2004. Localization accuracy in single-molecule microscopy. *Biophys. J.* 86:1185–1200. https://doi.org/10.1016/S0006-3495(04)74193-4.

14. Kay, S. M. 1993. Fundamentals of Statistical Signal Processing. *In* Estimation Theory, *Volume I.* Prentice Hall.

15. Smith, C. S., N. Joseph, B. Rieger, and K. A. Lidke. 2010. Fast, single-molecule localization that achieves theoretically minimum uncertainty. *Nat. Methods.* 7:373–375. https://doi.org/10.1038/nmeth.1449.

16. Weber, M., M. Leutenegger, S. Stoldt, S. Jakobs, T. S. Mihaila, A. N. Butkevich, and S. W. Hell. 2021. MINSTED fluorescence localization and nanoscopy. *Nat. Photonics.* 15:361–366. https://doi.org/10.1038/s41566-021-00774-2.

17. Van Trees, H. L. 2004. Detection, Estimation, and Modulation Theory, Part I: Detection, Estimation, and Linear Modulation Theory. John Wiley & Sons.

18. Gill, R. D., and B. Y. Levit. 1995. Applications of the van Trees inequality: a bayesian cramér-rao bound. *Bernoulli.* 1:59. https://doi.org/10.2307/3318681.

19. Masullo, L. A., L. F. Lopez, and F. D. Stefani. 2022. A common framework for single-molecule localization using sequential structured illumination. *Biophys. Rep.* 2:100036. https://doi.org/10.1016/j.bpr.2021.100036.

20. Fritsche, C., E. Özkan, L. Svensson, and F. Gustafsson. 2014. A fresh look at Bayesian Cramér-Rao bounds for discrete-time nonlinear filtering. *In* 17th International Conference on Information Fusion (FUSION), pp. 1–8.

21. Bay, S., C. Herzet, J.-M. Brossier, J.-P. Barbot, and B. Geller. 2008. Analytic and asymptotic analysis of bayesian cramér–rao bound for dynamical phase offset estimation. *IEEE Trans. Signal. Process.* 56:61–70. https://doi.org/10.1109/tsp.2007.906760.

22. Smith, C. S., K. Jouravleva, M. Huisman, S. M. Jolly, P. D. Zamore, and D. Grunwald. 2019. An automated Bayesian pipeline for rapid analysis of single-molecule binding data. *Nat. Commun.* 10:272. https://doi.org/10.1038/s41467-018-08045-5.

23. Levenberg, K. 1944. A method for the solution of certain non-linear problems in least squares. *Q. Appl. Math.* 2:164–168. https://doi.org/10.1090/qam/10666.

24. Marquardt, D. W. 1963. An algorithm for least-squares estimation of nonlinear parameters. *J. Soc. Ind. Appl. Math.* 11:431–441. https://doi.org/10.1137/0111030.

25. Kalisvaart, D., J. Cnossen, S.-T. Hung, S. Stallinga, M. Verhaegen, and C. S. Smith. 2022. Software Underlying: Precision in Iterative Modulation Enhanced Single-Molecule Localization Microscopy. https://github.com/qnano/iterative-localization.

26. Kalisvaart, D., J. Cnossen, S.-T. Hung, S. Stallinga, M. Verhaegen, and C. S. Smith. 2022. Data Underlying: Precision in Iterative Modulation Enhanced Single-Molecule Localization Microscopy. https://doi.org/10.4121/19786735.

27. Robert, C. P., and G. Casella. 2004. Monte Carlo Statistical Methods. Springer New York. https://doi.org/10.1007/978-1-4757-4145-2.

28. Hammersley, J. M. 1979. Monte Carlo Methods. Chapman and Hall.